Brain Structure and Function (2018) 223:3681–3688
https://doi.org/10.1007/s00429-018-1718-x

ORIGINAL ARTICLE

White matter tract anatomy in the rhesus monkey: a fiber dissection study

Thomas Decramer[1,2] · Stijn Swinnen[1] · Johannes van Loon[1] · Peter Janssen[2] · Tom Theys[1]

Received: 24 January 2018 / Accepted: 12 July 2018 / Published online: 18 July 2018

Abstract

Brain connectivity in non-human primates (NHPs) has been mainly investigated using tracer techniques and functional connectivity studies. Data on structural connections are scarce and come from diffusion tensor imaging (DTI), since gross anatomical white matter dissection studies in the NHP are lacking. The current study aims to illustrate the course and topography of the major white matter tracts in the macaque using Klingler's fiber dissection. 10 hemispheres obtained from 5 primate brains (*Macaca mulatta*) were studied according to Klingler's fiber dissection technique. Dissection was performed in a stepwise mesial and lateral fashion exposing the course and topography of the major white matter bundles. Major white matter tracts in the NHP include the corona radiata, tracts of the sagittal stratum, the uncinate fasciculus, the cingulum and the fornix. Callosal fiber topography was homologous to the human brain with leg motor fibers running in the posterior half of the corpus callosum. The relative size of the anterior commissure was larger in the NHP. NHPs and humans share striking homologies with regard to the course and topography of the major white matter tracts.

Keywords White matter · Klingler · Macaca mulatta · Neuroanatomy

Introduction

In neuroscience an important paradigm shift took place from a rigid topological brain organization towards a more dynamic interconnected network, the so-called connectome (Catani et al. 2012; De Benedictis and Duffau 2011; Sporns et al. 2005). This network view has yielded new insights regarding brain function (Mandonnet et al. 2007, 2009), plasticity (Duffau 2017) as well as pathogenesis and treatment of neurological diseases (Catani 2007; Catani et al. 2016; Ffytche and Catani 2005; Geschwind 1965a, b; Mesulam 1990, 2005). A major contributor to this shift was the development of diffusion tensor imaging (DTI), the first in vivo technique to visualize white matter tracts in the human brain. The rise of DTI subsequently caused a revival of older postmortem anatomical fiber dissection techniques, in particular Klingler's technique (Klingler 1935; Ludwig and Klingler 1956) as a means of validation (Burks et al. 2017; Latini et al. 2017; Martino et al. 2013).

Growing interest in functional brain connectivity led to advanced research in animal models, especially non-human primates (NHPs), whose brains share many structural and functional similarities with the human brain. Novel techniques such as functional magnetic resonance imaging (fMRI) combined with intracortical microstimulation can elucidate such neural networks, in an attempt to link structure and function (Petkov et al. 2015; Premereur et al. 2016).

White matter connections in monkeys have been demonstrated through lesion studies (Pandya et al. 1971a, b; Pandya and Kuypers 1969; Pandya and Vignolo 1971), tracer studies and more recently with the use of DTI (Adluru et al. 2012; Calabrese et al. 2015; Feng et al. 2017; Zakszewski et al. 2014; Zhang et al. 2013) and diffusion spectrum imaging (DSI) (Schmahmann et al. 2007). These techniques however result in an indirect visualization of white matter tracts, whereas anatomical fiber dissections make it possible to directly visualize the anatomical connections, i.e., the white matter bundle orientation and topography. Klingler's

Thomas Decramer and Stijn Swinnen contributed equally to this work.

✉ Thomas Decramer
thomas.decramer@kuleuven.be

[1] Laboratory for Experimental Neurosurgery and Neuroanatomy, KU Leuven, Leuven, Belgium

[2] Laboratory for Neuro- en Psychophysiology, KU Leuven, Leuven, Belgium

dissections have been extensively performed over the last decades, to describe white matter anatomy in the human brain (Baydin et al. 2017; Kucukyuruk et al. 2014; Naets et al. 2015; Peuskens et al. 2004; Ribas et al. 2017; Verhaeghe et al. 2018).

To our knowledge, this is the first report of white matter tract dissections using Klingler's technique in monkeys.

Materials and methods

Five rhesus monkey (*Macaca mulatta*) brains were fixed in a formalin aqueous solution (10%) for at least 4 weeks, and subsequently frozen for 2 additional weeks at − 15 °C, after which the specimens were allowed to thaw for several days in cold water. Brains were dissected according to the fiber dissection technique as described by Klingler (1935), Ludwig and Klingler (1956) and Naets et al. (2015). Joseph Klingler: "*We have imagined the action of the freezing to be as follows. The aqueous formol solution does not penetrate the myelinated nerve fibers, or only little; it is to be found more between the fibers, and the main masses of ice crystals arise in the latter location. Since water increases 10% in volume with the formation of ice, the fibers are somewhat spread apart. It is this loosening of tissue, which not only makes following of fine fiber bundles easier but in fact makes it possible at all*". After thawing and before the dissection was initiated, meticulous attention was paid to surface anatomy. Specimens were sharply divided at the midsagittal plane along the corpus callosum. The entire cortex was removed using a curved watchmaker's forceps until the short association fibers, the so-called U-fibers connecting adjacent gyri were exposed. A stepwise progressive mesial, lateral and inferior dissection followed, isolating fiber bundles in their glial sheets. Table 1 summarizes the dissection approach and tracts for all specimens. Dissections were performed under magnification with the aid of forceps and blunt spatulas. The thickness of the anterior commissure, defined as the largest diameter at the midsagittal plane, was measured using in vivo anatomical MRI scans (T1 MPRAGE sequence) in both rhesus monkeys (Siemens Trio, 3 T, isotropic voxel size 0.6 mm, TR 7.8 ms, TE 3.8 ms) and human subjects (Philips Achieva, 3 T, isotropic voxel size 1 mm, TR = 9.6 ms, TE = 4.6 ms).

To study the topography of callosal fibers, in particular homotopic motor fibers (Naets et al. 2015), the corpus callosum (CC) was segmented according to Witelson's division whereby the CC is partitioned into 7 segments (Witelson 1989).

Mesial and ventral dissections were performed in the same manner as previously described in human specimens (Naets et al. 2015; Peuskens et al. 2004; Verhaeghe et al. 2018).

Results

Macroscopic appearance and sulcal anatomy

Two hemispheres showed superficial cortical lesions after previous micro-electrode recording experiments; in one hemisphere an occipital abscess cavity was present. In all 10 specimens, we were able to macroscopically discern principal gyri and sulci.

On the lateral surface (Fig. 1a), the central sulcus (CS) separates the frontal lobe from the parietal lobe and extends ventrally almost to the lateral sulcus (LS). In the frontal lobe, the principal sulcus (PS) extends from the frontal pole towards the spur of the arcuate sulcus (AS). The superior temporal sulcus (STS) lies inferior and parallel to the lateral sulcus and continues posteriorly towards the inferoposterior border of the parietal lobe. In the parietal lobe, the intraparietal sulcus (IPS) separates the posterior parietal cortex into the superior and inferior parietal lobule. The occipital lobe houses the lunate sulcus (LuS) and the inferior occipital sulcus (IOS), which separates the temporal and the occipital lobe at their inferolateral surface.

Table 1 Overview of dissection approach and tracts

	Hemisphere	Approach	Tract
Monkey 1	Left	Lateral	SLF I/II/III, IC, UF, ILF, OR, iFOF, AC
	Right	Medial	CC, Cing
Monkey 2	Left	Lateral, medial	IC, UF, ILF, OR, iFOF, AC, CC, Cing
	Right	Medial, ventral	CC, Cing, ILF, OR, OT
Monkey 3	Left	Lateral	IC, UF, OR, AC
	Right	Medial	CC, Cing, sFOF
Monkey 4	Left	Lateral	SLF I/II/III, IC, UF, OR, iFOF, AC
	Right	Medial	CC, Cing, sFOF
Monkey 5	Left	Lateral	IC, UF, OR, iFOF, AC
	Right	Medial, ventral	CC, Cing, ILF, OR, OT

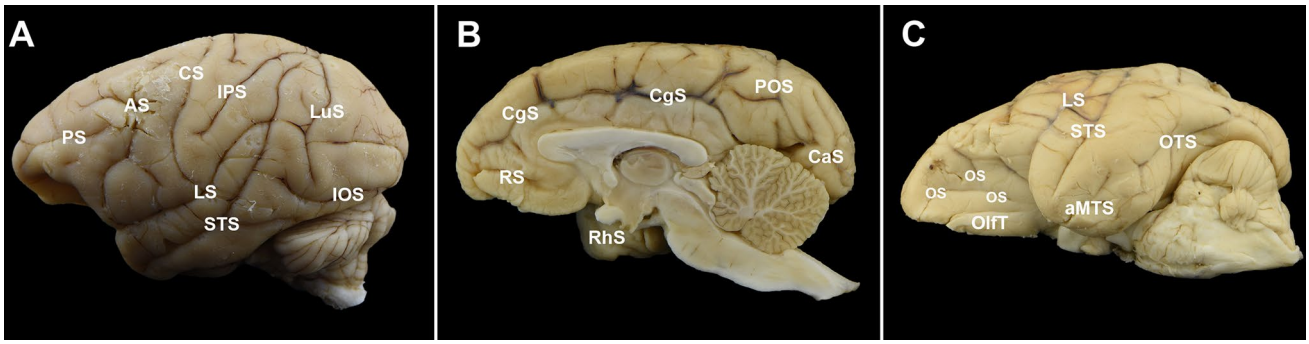

Fig. 1 Surface neuroanatomy. **a** Lateral surface. *AS* arcuate sulcus, *CS* central sulcus, *IOS* inferior occipital sulcus, *IPS* intraparietal sulcus, *LS* lateral sulcus, *LuS* lunate sulcus, *PS* principal sulcus, *STS* superior temporal sulcus. **b** Medial surface. *CaS* calcarine sulcus, *CgS* cingulate sulcus, *POS* parieto-occipital sulcus, *RS* rostral sulcus, *RhS* rhinal sulcus. **c** Ventral surface. *AMTS* anterior medial temporal sulcus, *LS* lateral sulcus, *OlfT* olfactory tract, *OS* orbital sulci, *OTS* occipitotemporal sulcus, *STS* superior temporal sulcus

On the mesial side (Fig. 1b) of the occipital lobe the calcarine sulcus (CaS) is found, while the parieto-occipital sulcus (POS) marks the border with the mesial parietal lobe. Further anteriorly, the cingulate gyrus is bordered by the callosal sulcus and the cingulate sulcus (CgS). Ventral to the CgS, the rostral sulcus (RS) is seen.

The ventral surface (Fig. 1c) of the frontal lobe contains the orbitofrontal cortex with the olfactory sulcus and the orbital sulci. On the ventral temporal surface, the occipitotemporal sulcus (OTS), the anterior and posterior medial temporal sulcus (AMTS, PMTS) and the rhinal sulcus (RhS) are visible.

Lateral dissection

The dissection was initiated in a lateral fashion with blunt removal of the gray matter. After peeling of the cortical surface, the arcuate or U-fibers looping around the different sulci connecting adjacent gyri are exposed (Fig. 2a). During removal of the U-fibers, longer association tracts can be

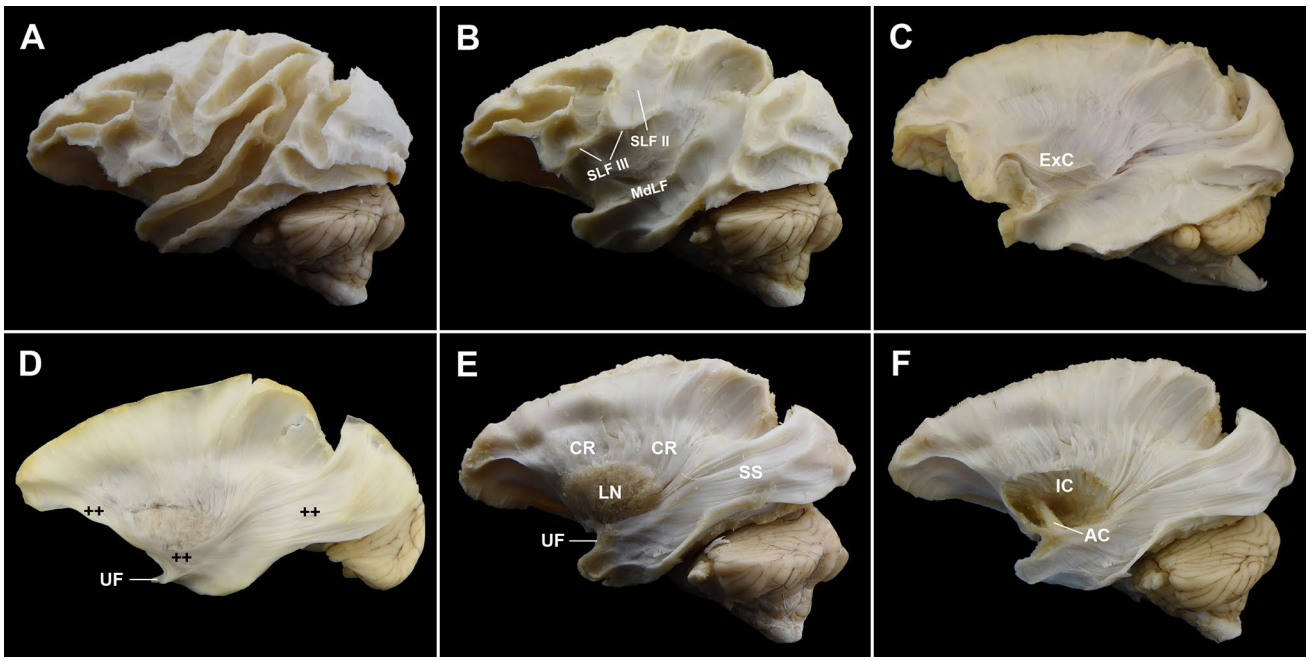

Fig. 2 Lateral dissection: progressive steps. **a** U-fibers (after removal of the gray matter). **b** During removal of the U-fibers the branches of the superior longitudinal fasciculus (SLF II, III) and the middle longitudinal fasciculus (MdLF) are exposed. **c** After removal of the U-fibers, the plane of the extreme capsule (ExC) is entered. **d, e** Progressive dissection reveals the lentiform nucleus (LN), the corona radiata (CR) and the sagittal stratum (SS). **f** *AC* anterior commissure *CR* corona radiata, *IC* internal capsule, *iFOF* inferior fronto-occipital fasciculus (++), *SS* sagittal stratum, *UF* uncinate fasciculus

appreciated (Fig. 2b). Inferior to the LS, in the white matter of the superior temporal gyrus the middle longitudinal fasciculus (MdLF) is coursing towards the inferior parietal lobule. Superior to the LS, white matter laminae comprising the second and third branches of the superior longitudinal fasciculus (SLF II, III) are connecting the inferior parietal lobule and the frontal lobe, with the SLF II being more medial and dorsal compared to the SLF III. The most dorsal branch, the SLF I is connecting the superior frontal gyrus (SFG) with the parietal lobe and can be encountered during either lateral or mesial dissection of the SFG (see below). At the level of the LS, upon removal of the superficial white matter laminae, the hidden insula can be revealed when the plane of the extreme capsule (ExC) is entered (Fig. 2c). Removal of the extreme capsule and claustrum leads to the external capsule (EC). Passing ventral to the anterior insula, at the limen, the hook-shaped uncinate fasciculus (UF) connects the anterior temporal lobe with the orbitofrontal cortex (Fig. 2d, e).

After removal of the superficial association fibers, the corona radiata and the sagittal stratum (SS) are readily exposed (Fig. 2d–f). The bundles comprising the SS form a sagittal white matter plane in the posterior lobes and consists of anatomically closely associated fibers of the optic radiation, the inferior longitudinal fasciculus (ILF) and the putative inferior fronto-occipital fasciculus (iFOF). The ILF courses between the occipital and the anterior temporal lobe; during the ventral dissection (see below) its connections with the ventral and mesial temporal areas can be appreciated. The fibers of the iFOF have a characteristic sigmoid shape and interconnect the occipital and the ventral frontal lobe. This bundle converges at the level of the external capsule in a region shared with the UF and becomes compact just dorsal to the UF (Fig. 3).

Removal of the EC leads to the lentiform nucleus (LN), where the fibers of the corona radiata converge and penetrate the internal capsule (IC) (Fig. 2e). After removal of the LN, the IC and the anterior commissure (AC) are revealed (Fig. 2f).

The AC forms a large compact bundle that interconnects both temporal lobes. The relative size of the AC was remarkable and appeared disproportionately larger compared to the human AC. We therefore performed additional measurements on anatomical MRI in 11 monkeys (2F:9M) and 11 human subjects (6F:5M) to compare the maximal diameter at the midsagittal plane. In humans, we found an average AC diameter of 3.0 (±0.53 mm), in the monkey the AC averaged 2.5 (±0.34) mm (Fig. 4).

Mesial dissection

Landmarks for the mesial dissection are the corpus callosum (CC), the cingulate gyrus, the thalamus (Th), the septum pellucidum (SP), the third ventricle (III), the fornix (Fo), the optic chiasm (OC), the AC and the posterior commissure (PC).

After blunt removal of the gray matter and short U-fibers, the region of the SLF I and the cingulum (Cing) are exposed (Fig. 5a). The cingulate part of the Cing is covered by the cingulate cortex and follows a C-shaped trajectory around the CC, where at the level of the splenium it sweeps inferiorly and laterally continuing as the hippocampal part of the Cing. Removal of the Cing exposes the radiation of the CC (Fig. 5b). The course of the interconnecting callosal fibers from the medial motor areas can be tracked and their crossing at the midline can be marked.

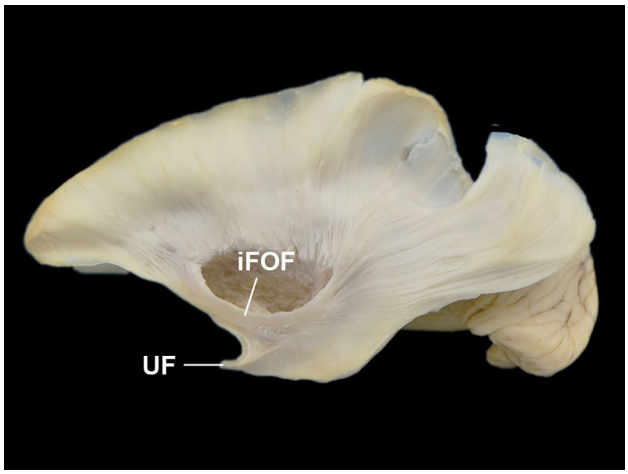

Fig. 3 Putative inferior frontoccipital fasciculus (iFOF). After removal of the lentiform nucleus (LN), the course of the putative iFOF is shown. The UF can be appreciated ventral to this tract

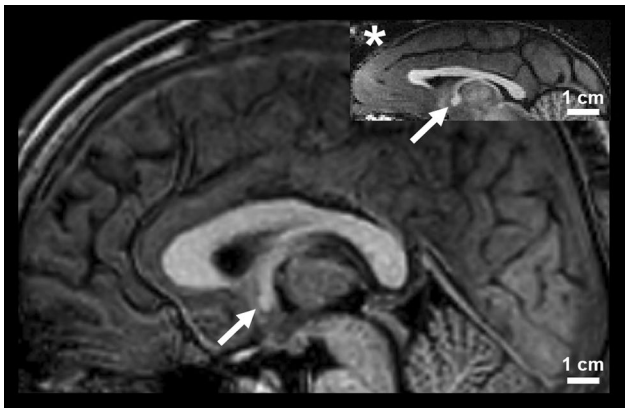

Fig. 4 Human vs macaque MRI scan at the midsagittal plane. The disproportionate size of the anterior commissure (AC) (arrow) relative to the brain size in the macaque (*) is illustrated. Figures are scaled according to the average cerebrum length for both species according to Corthout (2014)

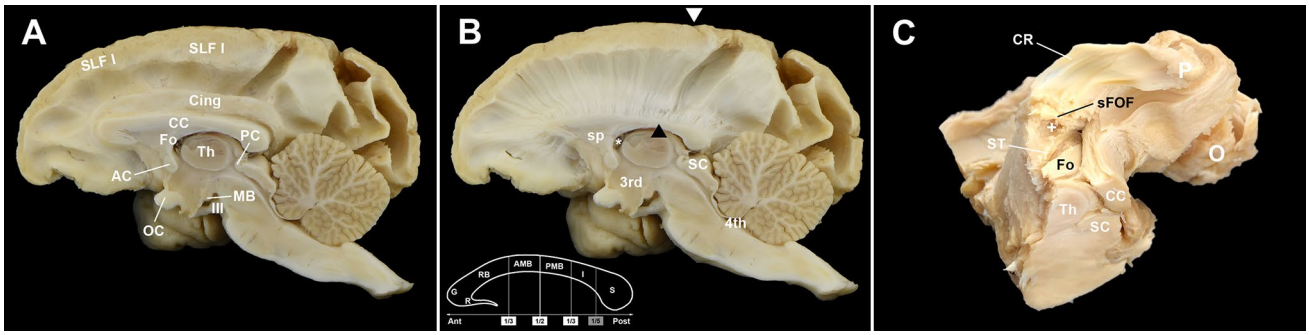

Fig. 5 Mesial dissection. **a** Mesial anatomy after removal of the gray matter. *III* oculomotor nerve, *MB* mammillary Body, *OC* optic chiasm, AC anterior commissure, *Th* thalamus, *PC* posterior commissure, *Fo* fornix, *CC* corpus callosum, *Cing* cingulum, *SLF* I superior longitudinal fasciculus subcomponent I. **b** After removal of the cingulum and surrounding U-fibers, the callosal radiation is exposed. The white arrowhead represents the central sulcus. The crossing of the callosal fibers from the depth of the central sulcus is marked by the black arrowhead. Callosal leg motor fibers run in the isthmus and posterior midbody of the CC. *3rd* third ventricle, *4th* fourth ventricle, * foramen of Monro, *SC* superior colliculus, *sp* septum pellucidum. Small insert shows Witelson's classification of the CC: *R* rostrum, *G* genu, *RB* rostral body, *AMB* anterior midbody, *PMB* posterior midbody, *I* isthmus, *S* splenium. **c** Coronal section through thalamus and brainstem, superior–anterior view. + tail of caudate nucleus, *CR* corona radiata, *O* occipital lobe, *P* parietal lobe, *sFOF* superior fronto-occipital fasciculus, *ST* stria terminalis

These callosal motor fibers invariantly cross the midline in the posterior half of the CC (Fig. 5b).

To study the paramedian subcallosal region, a coronal section at the level of the thalamus and brainstem was made after exposing the corona radiata (through both a lateral and mesial white matter dissection). The body of the caudate nucleus (CN) was removed after which the isthmus of the CC was dissected. An antero-posteriorly orientated white matter tract, corresponding to the superior fronto-occipital fasciculus (sFOF) (Forkel et al. 2014; Schmahmann and Pandya 2006) was identified in the subcallosal area medial to the corona radiata and superolateral to the caudate nucleus (Fig. 5c). In Fig. 5c, the stria terminalis is also depicted and travels medial to the caudate nucleus.

Ventral dissection

The smaller orbitofrontal sulci are visible after blunt removal of the gray matter of the frontal lobe (Fig. 6a). Upon removal of the inferior temporal cortex the impression of the major sulci, in particular the STS and OTS can be discerned, after which the plane of the ILF is entered (Fig. 6a). Continuing the dissection more medially exposes the amygdala, hippocampus and temporal horn of the lateral ventricle. The ILF, the anterior temporal lobe as well as the hippocampus are removed after which the optic tract (OT) is visualized coursing towards the lateral geniculate body (LGN). The geniculo-calcarine tract or optic radiation (OR) sweeps along the lateral wall of the lateral ventricle before reaching the occipital cortex.

Discussion

This study provides insights into the connectional neuroanatomy of the rhesus monkey. Klingler's fiber dissection is feasible in the macaque (*Macaca mulatta*) and the technique provides an elegant method to illustrate the anatomical organization of the white matter pathways. We demonstrate that the course and topography of the major fiber tracts in the NHP is remarkably similar to the human brain.

Although the sulcal pattern of the monkey brain differs substantially from humans, the appearance of the major commissural, projection and association tracts shows many homologies between both species. Certain issues however warrant further discussion.

Since the monkey brain is dramatically smaller (95 g) than the human brain (1350 g), the dissection and visualization of certain long association tracts, in particular the different branches of the SLF, are much harder since these bundles only represent tiny white matter sheets overlying the corona radiata. It is therefore impossible to clearly visualize individual fibers from these superficial association tracts. Previous studies have furthermore shown that the SLF in macaque monkeys is less well-developed in comparison to humans (Rilling et al. 2008). Larger fiber tracts such as the corona radiata, the fornix, the stria terminalis, the cingulum and the uncinate fasciculus can be easily identified and take a similar course in both species.

Interspecies dissimilarities exist regarding the fronto-occipital fiber (FOF) system. Though the human iFOF represents a clear and distinct white matter bundle, the existence of a human sFOF remains controversial. The

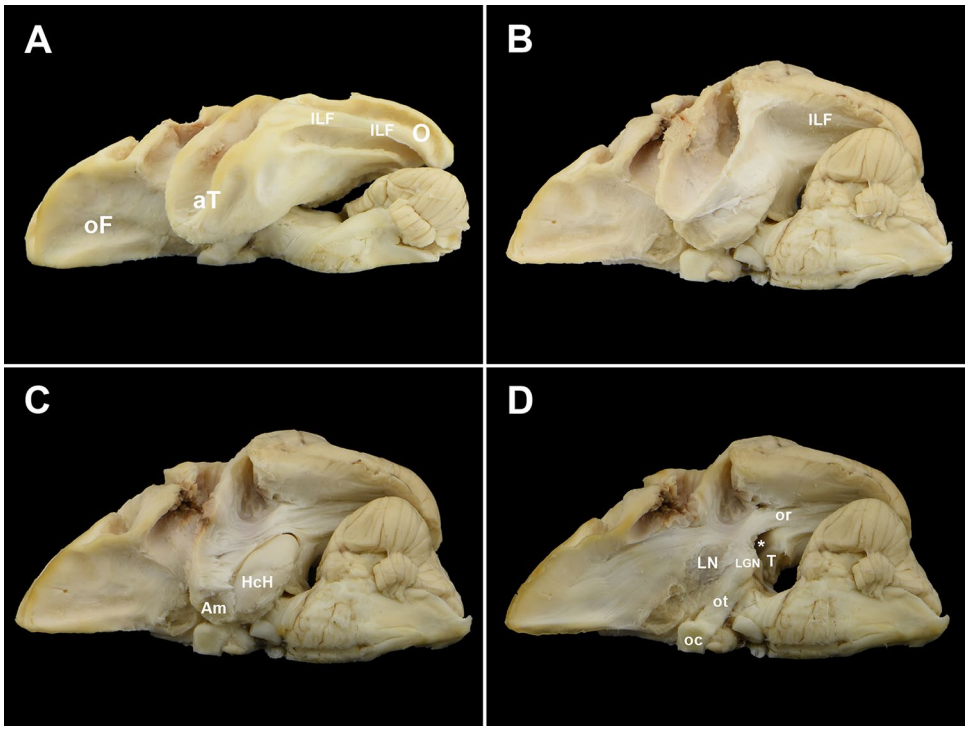

Fig. 6 Ventral dissection. **a, b** After removal of the gray matter, the U-fibers are exposed. *aT* anterior temporal, *O* occipital, *oF* orbitofrontal, *ILF* inferior longitudinal fasciculus. **c** Removal of the medial temporal white matter leads to the temporal horn of the lateral ventricle with the head of the hippocampus (*HcH*). **d** Inferior view after hippocampal removal. *LGN* lateral geniculate nucleus, *LN* lentiform nucleus, *oc* optic chiasm, *or* optic radiation, *ot* optic tract, *T* tail of hippocampus, * atrium of lateral ventricle

sFOF is seen in humans with congenital agenesis of the corpus callosum (Forkel et al. 2014) but might not be present in healthy human brains (Meola et al. 2015; Thiebaut de Schotten et al. 2012). In monkeys on the other hand, the superior fronto-occipital fasciculus (sFOF) represents an association tract between the CC and the corona radiata (Schmahmann and Pandya 2006), while the iFOF has not been described in NHPs (Forkel et al. 2014; Schmahmann and Pandya 2006; Schmahmann et al. 2007; Takemura et al. 2017). In the majority of dissections, we encountered an inferior fronto-occipital tract, with a course very similar to the iFOF in humans. The existence of a putative monkey iFOF is also supported by recent DTI studies (Feng et al. 2017; Mars et al. 2016). Identification of the iFOF in the NHP is however difficult since the tract clearly appears smaller in comparison to the human brain and since its course can be difficult to interpret as it joins the UF in the temporal stem. The inherent limitations of Klinger's technique which represents a macroscopic dissection tool make strong statements on smaller white matter tracts (such as SLF and iFOF) more difficult.

A matter of debate in the literature concerns the inferior longitudinal fascicle (ILF), this bundle was first described as a distinct white matter pathway using blunt dissection. This idea was challenged by Tusa and Ungerleider (1985) who described the ILF as a series of U-fibers connecting striate and extrastriate visual areas, they did not find evidence of cortico-cortical connections between occipital and temporal cortex within the sagittal stratum in monkeys and humans. More recent DTI (Catani et al. 2003; Feng et al. 2017) and tracer studies (Schmahmann and Pandya 2006) however describe the ILF as a distinct white matter pathway, apart from a well-developed U-fiber projection system between these cortical areas. Our dissections did not show a clear distinction between a single long white matter pathway and a well-developed U-fiber projection system, in accordance with previous human dissection studies where the term inferior longitudinal projection system (ILPS) was coined (Peuskens et al. 2004).

Interspecies similarities and dissimilarities extend to the commissural system. Although lesion studies in monkeys suggested a more anterior position of the callosal motor fibers compared to the human brain (Pandya et al. 1971b), possibly due to an extensive prefrontal development in humans (with callosal motor fibers pushed backward), a DTI study has shown that the location of the callosal motor fibers in NHPs is very similar to humans (Hofer et al. 2008). Although the absolute size of the human frontal cortex is larger compared to other primates, the frontal cortex in humans and macaque monkeys occupies a comparable portion of the cortex of the cerebral hemisphere (38 vs 31%) (Semendeferi et al. 2002). The callosal radiation in our NHP dissections appeared very similar to human specimens (Naets et al. 2015) with a callosal fiber distribution following roughly the same pattern in both species. A clear dissimilarity in both species is the relative size of the anterior commissure, which is larger in the NHP In humans, we found an average AC diameter

of 3.0 (± 0.53 mm), in the monkey the AC averaged 2.5 (± 0.34) mm, which is disproportionate to the size of the brain of both species [macaque vs human: cerebrum length 7.5 vs 17 cm, cerebral surface area 100 vs 1000 cm^2 and cerebral volume 70 vs 1100 cm^3 (Corthout 2014)] (Fig. 4). From an evolutionary perspective, the CC is a relatively recent development and exclusive to placental mammals (Katz et al. 1983; Mihrshahi 2006). While representing the principal commissure in non-mammalians (Ashwell et al. 1996; Heath and Jones 1971) the relative role of the AC as a commissural pathway has diminished during evolution. In the monkey the AC mainly connects the temporal and orbitofrontal cortex.

Klingler's dissection technique has several limitations. Although white matter tract orientation and course can be identified using the technique, visualizing exact tract termination can be more problematic. Tracer studies are complementary in this respect, since they allow to study precise projections without the anatomical tract information DTI and Klingler's dissection provide. Klingler's technique therefore remains a qualitative analysis of white matter tract anatomy which is dependent on the quality of dissection. Results cannot be described in a quantitative manner. In particular for non-human primates, the small brain size and thickness of the white matter tracts makes the dissection more difficult compared to the human brain.

Although the size and sulcal anatomy of the NHP brain is very different from human brains, the current data complement earlier imaging and tracer studies on the similarities of the white matter pathways in both species. These findings can be important for future anatomical and functional connectivity studies.

Acknowledgements This work was supported by the Department of Neurosurgery, Klinisch Onderzoeks Fonds (KOF, UZ Leuven) and Project financiering KU Leuven. We thank Jo Verbinnen and Kristof Reyniers for technical assistance. Tom Theys is a Senior Clinical Investigator of Fonds Wetenschappelijk Onderzoek (FWO) Flanders (FWO 1830717N).

Funding This work was supported by the Department of Neurosurgery, Klinisch Onderzoeks Fonds (KOF, UZ Leuven) and Project financiering KU Leuven. Tom Theys is a Senior Clinical Investigator of FWO Flanders (FWO 1830717N).

Compliance with ethical standards

Conflict of interest All authors report no conflict of interest.

Ethical approval The study was approved by the Animal Ethics Committee, KU Leuven, Belgium.

Animal welfare statement All applicable international, national, and/or institutional guidelines for the care and use of animals were followed. All procedures performed in studies involving animals were in accordance with the ethical standards of the institution or practice at which the studies were conducted.

References

Adluru N et al (2012) A diffusion tensor brain template for rhesus macaques. NeuroImage 59:306–318 https://doi.org/10.1016/j.neuroimage.2011.07.029

Ashwell KW, Marotte LR, Li L, Waite PM (1996) Anterior commissure of the wallaby (*Macropus eugenii*): adult morphology and development. J Comp Neurol 366:478–494. https://doi.org/10.1002/(SICI)1096-9861(19960311)366:3%3C478::AID-CNE8%3E3.0.CO;2-1

Baydin S, Gungor A, Tanriover N, Baran O, Middlebrooks EH, Rhoton AL Jr (2017) Fiber tracts of the medial and inferior surfaces of the cerebrum. World Neurosurg 98:34–49. https://doi.org/10.1016/j.wneu.2016.05.016

Burks JD et al (2017) Anatomy and white matter connections of the orbitofrontal gyrus. J Neurosurg. https://doi.org/10.3171/2017.3.JNS162070

Calabrese E, Badea A, Coe CL, Lubach GR, Shi Y, Styner MA, Johnson GA (2015) A diffusion tensor MRI atlas of the postmortem rhesus macaque brain. NeuroImage 117:408–416 https://doi.org/10.1016/j.neuroimage.2015.05.072

Catani M (2007) From hodology to function. Brain J Neurol 130:602–605. https://doi.org/10.1093/brain/awm008

Catani M, Jones DK, Donato R, Ffytche DH (2003) Occipito-temporal connections in the human brain. Brain J Neurol 126:2093–2107. https://doi.org/10.1093/brain/awg203

Catani M et al (2012) Beyond cortical localization in clinico-anatomical correlation. Cortex J Devot Stud Nerv Syst Behav 48:1262–1287. https://doi.org/10.1016/j.cortex.2012.07.001

Catani M et al (2016) Frontal networks in adults with autism spectrum disorder. Brain J Neurol 139:616–630. https://doi.org/10.1093/brain/awv351

Corthout EC (2014) The eye and brain in macaque and man: linear, areal and volumetric dimensions. Acco, Lake Zurich

De Benedictis A, Duffau H (2011) Brain hodotopy: from esoteric concept to practical surgical applications. Neurosurgery 68:1709–1723. https://doi.org/10.1227/NEU.0b013e3182124690 **(discussion 1723)**

Duffau H (2017) Hodotopy, neuroplasticity and diffuse gliomas. Neurochirurgie 63:259–265. https://doi.org/10.1016/j.neuchi.2016.12.001

Feng L et al (2017) Population-averaged macaque brain atlas with high-resolution ex vivo DTI integrated into in vivo space. Brain Struct Funct 222:4131–4147. https://doi.org/10.1007/s00429-017-1463-6

Ffytche DH, Catani M (2005) Beyond localization: from hodology to function. Philos Trans R Soc Lond Ser B Biol Sci 360:767–779. https://doi.org/10.1098/rstb.2005.1621

Forkel SJ, Thiebaut de Schotten M, Kawadler JM, Dell'Acqua F, Danek A, Catani M (2014) The anatomy of fronto-occipital connections from early blunt dissections to contemporary tractography. Cortex J Devot Stud Nerv Syst Behav 56:73–84. https://doi.org/10.1016/j.cortex.2012.09.005

Geschwind N (1965a) Disconnexion syndromes in animals and man. I. Brain J Neurol 88:237–294

Geschwind N (1965b) Disconnexion syndromes in animals and man. II. Brain J Neurol 88:585–644

Heath CJ, Jones EG (1971) Interhemispheric pathways in the absence of a corpus callosum. An experimental study of commissural connexions in the marsupial phalanger. J Anat 109:253–270

Hofer S, Merboldt KD, Tammer R, Frahm J (2008) Rhesus monkey and human share a similar topography of the corpus callosum as revealed by diffusion tensor MRI in vivo. Cereb Cortex 18:1079–1084 https://doi.org/10.1093/cercor/bhm141

Katz MJ, Lasek RJ, Silver J (1983) Ontophyletics of the nervous system: development of the corpus callosum and evolution of axon tracts. Proc Natl Acad Sci USA 80:5936–5940

Klingler J (1935) Erleichterung des makroskopischen Praeparation des Gehirns durch den Gefrierprozess. Schweiz Arch Neurol Psychiatr:247–256

Kucukyuruk B, Yagmurlu K, Tanriover N, Uzan M, Rhoton AL Jr (2014) Microsurgical anatomy of the white matter tracts in hemispherotomy. Neurosurgery 10 Suppl 2:305–324. https://doi.org/10.1227/NEU.0000000000000288 **(discussion 324)**

Latini F et al (2017) Segmentation of the inferior longitudinal fasciculus in the human brain: a white matter dissection and diffusion tensor tractography study. Brain Res 1675:102–115. https://doi.org/10.1016/j.brainres.2017.09.005

Ludwig E, Klingler J (1956) Atlas cerebri humani. Karger, Basel

Mandonnet E, Nouet A, Gatignol P, Capelle L, Duffau H (2007) Does the left inferior longitudinal fasciculus play a role in language? A brain stimulation study. Brain J Neurol 130:623–629. https://doi.org/10.1093/brain/awl361

Mandonnet E, Gatignol P, Duffau H (2009) Evidence for an occipitotemporal tract underlying visual recognition in picture naming. Clin Neurol Neurosurg 111:601–605. https://doi.org/10.1016/j.clineuro.2009.03.007

Mars RB et al (2016) The extreme capsule fiber complex in humans and macaque monkeys: a comparative diffusion MRI tractography study. Brain Struct Funct 221:4059–4071. https://doi.org/10.1007/s00429-015-1146-0

Martino J, De Witt Hamer PC, Berger MS, Lawton MT, Arnold CM, de Lucas EM, Duffau H (2013) Analysis of the subcomponents and cortical terminations of the perisylvian superior longitudinal fasciculus: a fiber dissection and DTI tractography study. Brain Struct Funct 218:105–121. https://doi.org/10.1007/s00429-012-0386-5

Meola A, Comert A, Yeh FC, Stefaneanu L, Fernandez-Miranda JC (2015) The controversial existence of the human superior fronto-occipital fasciculus: connectome-based tractographic study with microdissection validation. Hum Brain Map 36:4964–4971. https://doi.org/10.1002/hbm.22990

Mesulam MM (1990) Large-scale neurocognitive networks and distributed processing for attention, language, and memory. Ann Neurol 28:597–613. https://doi.org/10.1002/ana.410280502

Mesulam M (2005) Imaging connectivity in the human cerebral cortex: the next frontier? Ann Neurol 57:5–7. https://doi.org/10.1002/ana.20368

Mihrshahi R (2006) The corpus callosum as an evolutionary innovation. J exp Zool Part B Mol Dev Evol 306:8–17. https://doi.org/10.1002/jez.b.21067

Naets W, Van Loon J, Paglioli E, Van Paesschen W, Palmini A, Theys T (2015) Callosotopy: leg motor connections illustrated by fiber dissection. Brain Struct Funct https://doi.org/10.1007/s00429-015-1167-8

Pandya DN, Kuypers HG (1969) Cortico-cortical connections in the rhesus monkey. Brain Res 13:13–36

Pandya DN, Vignolo LA (1971) Intra- and interhemispheric projections of the precentral, premotor and arcuate areas in the rhesus monkey. Brain Res 26:217–233

Pandya DN, Dye P, Butters N (1971a) Efferent cortico-cortical projections of the prefrontal cortex in the rhesus monkey. Brain Res 31:35–46

Pandya DN, Karol EA, Heilbronn D (1971b) The topographical distribution of interhemispheric projections in the corpus callosum of the rhesus monkey. Brain Res 32:31–43

Petkov CI, Kikuchi Y, Milne AE, Mishkin M, Rauschecker JP, Logothetis NK (2015) Different forms of effective connectivity in primate frontotemporal pathways. Nat Commun 6:6000. https://doi.org/10.1038/ncomms7000

Peuskens D, van Loon J, Van Calenbergh F, van den Bergh R, Goffin J, Plets C (2004) Anatomy of the anterior temporal lobe and the frontotemporal region demonstrated by fiber dissection. Neurosurgery 55:1174–1184

Premereur E, Taubert J, Janssen P, Vogels R, Vanduffel W (2016) Effective connectivity reveals largely independent parallel networks of face and body patches. Curr Biol 26:3269–3279. https://doi.org/10.1016/j.cub.2016.09.059

Ribas EC, Yagmurlu K, de Oliveira E, Ribas GC, Rhoton A Jr (2017) Microsurgical anatomy of the central core of the brain. J Neurosurg. https://doi.org/10.3171/2017.5.JNS162897

Rilling JK, Glasser MF, Preuss TM, Ma X, Zhao T, Hu X, Behrens TE (2008) The evolution of the arcuate fasciculus revealed with comparative DTI. Nat Neurosci 11:426–428. https://doi.org/10.1038/nn2072

Schmahmann J, Pandya D (2006) Fiber pathways of the brain. Oxford University Press, New York

Schmahmann JD, Pandya DN, Wang R, Dai G, D'Arceuil HE, de Crespigny AJ, Wedeen VJ (2007) Association fibre pathways of the brain: parallel observations from diffusion spectrum imaging and autoradiography. Brain J Neurol 130:630–653. https://doi.org/10.1093/brain/awl359

Semendeferi K, Lu A, Schenker N, Damasio H (2002) Humans and great apes share a large frontal cortex. Nature Neurosci 5:272–276. https://doi.org/10.1038/nn814

Sporns O, Tononi G, Kotter R (2005) The human connectome: a structural description of the human brain. PLoS Comput Biol 1:e42. https://doi.org/10.1371/journal.pcbi.0010042

Takemura H et al (2017) Occipital white matter tracts in human and macaque. Cereb Cortex 27:3346–3359. https://doi.org/10.1093/cercor/bhx070

Thiebaut de Schotten M, Dell'Acqua F, Valabregue R, Catani M (2012) Monkey to human comparative anatomy of the frontal lobe association tracts. Cortex J Devot Stud Nerv Syst Behav 48:82–96. https://doi.org/10.1016/j.cortex.2011.10.001

Tusa RJ, Ungerleider LG (1985) The inferior longitudinal fasciculus: a reexamination in humans and monkeys. Ann Neurol 18:583–591. https://doi.org/10.1002/ana.410180512

Verhaeghe A, Decramer T, Naets W, Van Paesschen W, van Loon J, Theys T (2018) Posterior quadrant disconnection: a fiber dissection study. Oper Neurosurg 14:45–50. https://doi.org/10.1093/ons/opx060

Witelson SF (1989) Hand and sex differences in the isthmus and genu of the human corpus callosum. A postmortem morphological study. Brain J Neurol 112(Pt 3):799–835

Zakszewski E, Adluru N, Tromp do PM, Kalin N, Alexander AL (2014) A diffusion-tensor-based white matter atlas for rhesus macaques. PLoS One 9:e107398. https://doi.org/10.1371/journal.pone.0107398

Zhang D et al (2013) Diffusion tensor imaging reveals evolution of primate brain architectures. Brain Struct Funct 218:1429–1450. https://doi.org/10.1007/s00429-012-0468-4